Title	The Origin of Spodumene Pegmatites Associated with the Leinster Granite in Southeast Ireland
Authors(s)	Barros, Renata; Menuge, Julian
Publication date	2016-07-01
Publication information	Canadian Mineralogist, 54 (4): 847-862
Publisher	Mineralogical Association of Canada
Item record/more information	http://hdl.handle.net/10197/11562
Publisher's version (DOI)	10.3749/canmin.1600027

THE ORIGIN OF SPODUMENE PEGMATITES ASSOCIATED WITH THE LEINSTER GRANITE IN SOUTHEAST IRELAND

RENATA BARROS
School of Earth Sciences, University College Dublin
Belfield, Dublin D04 N2E5, Ireland

JULIAN F. MENUGE
School of Earth Sciences, Earth Institute and iCRAG, University College Dublin
Belfield, Dublin D04 N2E5, Ireland

ABSTRACT

Rare-element pegmatites have diverse chemical signatures and are important sources of strategic metals such as Li, Cs and Ta. The two main hypotheses to explain rare-element pegmatite formation are 1) residual magmas from granitic rocks' crystallization, and 2) partial melts from a relatively rare-element-rich source. In southeast Ireland, spodumene and spodumene-free pegmatite dykes occur along the eastern margin of the S-type Leinster Granite batholith. With indistinguishable emplacement ages around 400 Ma, the origin of the Li-rich pegmatitic fluids has been suggested to have resulted from extreme fractional crystallization of Leinster Granite granodiorite magma. To test this hypothesis, we used whole-rock geochemistry of pegmatite and granodiorite samples from drill cores and geochemical modeling of *in situ* crystallization and batch melting to investigate which process better explains the formation of pegmatites. Chemical signatures for pegmatites and granodiorite do not indicate a direct comagmatic relationship, as granodiorite has higher concentrations of many incompatible elements than the pegmatites (*e.g.* concentrations of Zr, Ti and Y). Concentrations of Li, Rb, Cs, Sr and Ba show no clear fractionation trends from granodiorite to pegmatite. The *in situ* crystallization model using the average granodiorite composition as initial magma generates a range of compositions that does not include pegmatites, so it is unlikely that they represent residual granitic magmas. Modeling of partial melting indicates that Leinster Granite granodiorite and pegmatite magmas could have been formed in separate events and from chemically different source rocks, with pegmatite magmas presumably formed in a younger event because pegmatites intrude granodiorite.

KEYWORDS

Spodumene pegmatite; Leinster Granite; geochemical modeling; *in situ* crystallization; batch melting; petrogenesis.

INTRODUCTION

Rare-element pegmatites display very diverse chemical signatures and are enriched in elements that are usually present in low concentrations in other rocks. These features make them important sources of a wide range of commodities, including industrial minerals, gemstones and strategic metals. Two alternative petrogenetic processes have been proposed to explain the formation of rare-element pegmatites: 1) extensive fractionation of fertile parental granitic magma, with rare-element pegmatites representing the residual phase in this process; or 2) partial melting of rare-element-rich source rocks. Pegmatites geographically associated with granitic batholiths have often led to support for the first hypothesis that granitic rocks and pegmatite magmas have a comagmatic relationship. Several studies have successfully demonstrated the link between parent granite and pegmatites, including examples in Canada (Černý *et al.* 2012) and Spain (Roda-Robles *et al.* 2012). However age and/or geochemical incompatibilities, such as pegmatites being significantly older than granite, or an apparent absence of parental granite, are often documented (*e.g.* Walker *et al.* 1989, Muller *et al.* 2015).

One way to approach and resolve the petrogenetic problem is to use quantitative trace element modeling and mathematically test different models. We use this approach for a pegmatite belt in southeast Ireland, which is associated with the peraluminous Leinster Granite. A genetic link between them has been suggested based on age and geochemical similarities (O'Connor *et al.* 1991, Whitworth & Rankin 1989), but the exact relationship between them remains uncertain. As a result of new lithium exploration drilling being carried by Blackstairs Lithium Ltd., an extensive lithogeochemical database is available that provides drill core of the entire thickness of several pegmatite dykes. Coupled with textural and mineralogical observations on the drill core, these are used for geochemical modeling to better constrain the origin of these rare metal pegmatites.

GEOLOGICAL SETTING AND PREVIOUS STUDIES

The geology of the southeast of Ireland is dominated by Paleozoic basement and igneous intrusions (Fig. 1). The basement is composed of sedimentary and associated volcanic rocks regionally metamorphosed to lower greenschist facies and is subdivided into the following units and lithologies: greywacke and shale of the Cambrian Bray and Cahore Groups; mudstone, siltstone and sandstone of the Ordovician Ribband Group; deep marine shale, now commonly slate, with abundant intermediate to acidic volcanic rocks of the Ordovician Duncannon Group; and the deep marine turbidite sequence of the Silurian Leinster Inlier (Graham & Stillman 2009, Holland 2009).

The largest of the younger igneous intrusions is the Leinster Granite, a Caledonian batholith composed at least in part of sheeted intrusions (Grogan & Reavy 2002) of S-type two-mica granitic rocks (predominantly granodiorite) intruded into the metasedimentary basement. The batholith is part of the Trans-Suture Suite (Brown *et al.* 2008), which spans the trace of the Iapetus suture in Britain

and Ireland. According to the same authors, the origin of these granitic magmas is related to orogen-wide sinistral transtension during the early Devonian, triggering lamprophyre magma generated by melting of Avalonian lithospheric mantle to rise and transfer heat to the lower part of the Avalonian crust, forming partial melts with S-type granitic composition. The Leinster Granite comprises five plutons aligned with the NE-SW regional strike of the Lower Paleozoic supracrustal country rocks (McConnell & Philcox 1994). Despite its size, the batholith is poorly exposed. Most available data are from the better exposed Northern pluton, including a U-Pb monazite age of 405 ± 2 Ma (O'Connor *et al.* 1989). It has been assumed that all plutons intruded and crystallized simultaneously (Brindley 1973) and therefore that this age applies to the whole batholith. However a wide variability in initial Sr and Nd isotope ratios, both between and within plutons, has been interpreted as resulting from the generation of different magma batches by partial melting of an isotopically heterogeneous sedimentary source (Mohr 1991). In addition, disequilibrium textures in plagioclase phenocrysts indicate a multi-stage and multi-scale acid-acid mixing of magma batches during ascent and emplacement (Grogan & Reavy 2002).

A network of lithium pegmatite dykes, metres to tens of metres thick, is known from at least nine localities along the eastern margin of the Tullow Lowlands pluton and within the schist septum that separates it from the Blackstairs Unit to the south (Fig. 1). There are almost no outcrops of these dykes and the localities have been identified by concentrations of glacial boulders, in several cases confirmed by mineral exploration drilling (Steiger & von Knorring 1974, Steiger 1977). Most of the dykes so far detected roughly follow the NE-SW regional structure of the Caledonian East Carlow Deformation Zone (McArdle & Kennedy 1985). They intrude the Tullow pluton, minor granitic bodies related to the Leinster Granite and quartz-mica schist formed by contact metamorphism of the Leinster Granite with the Ribband Group. Rb-Sr isotope studies of the pegmatites (O'Connor *et al.* 1991) yielded a whole-rock errorchron age of 396 ± 7 Ma (MSWD = 5.54), constructed using spodumene pegmatites, associated lepidolite greisens and barren pegmatites. This corresponds to an age of 402 ± 7 Ma when recalculated using the recent IUGS recommendation on ^{87}Rb half life (Villa *et al.* 2015). The pegmatite errorchron initial Sr ratio of 0.705 ± 0.005 (O'Connor *et al.* 1991) lies within the Leinster Granite range obtained by Mohr (1991). Moreover, results from fluid inclusion analysis (Whitworth & Rankin 1989) and mineral chemistry (Whitworth 1992) suggest a genetic link between the Leinster Granite and lithium pegmatites. Despite the indistinguishable Caledonian ages of granitic rocks and pegmatites and their similar initial Sr isotope ratios, it is debatable whether lithium pegmatites represent the residual magma after crystallization of the Leinster Granite, or were formed from separate partial melts of similar or different metasedimentary sources. Here we aim to better constrain the petrogenesis of the pegmatite belt and its relationship with the Leinster Granite.

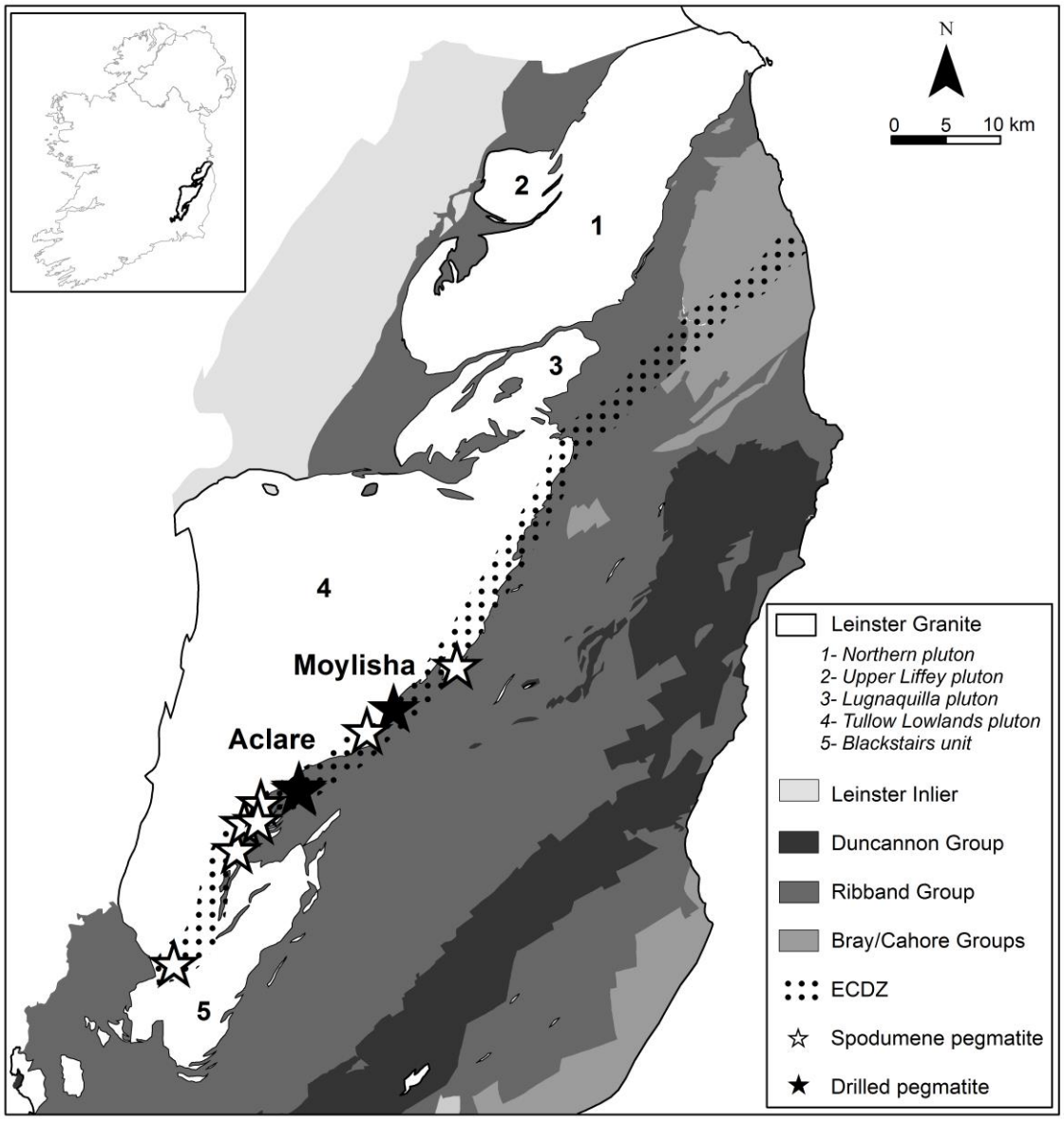

Fig 1: Spodumene pegmatite occurrences in southeast Ireland. Dykes are restricted to the eastern margin of the Tullow Lowlands pluton, spatially associated with the East Carlow Deformation Zone (ECDZ). Pegmatites intrude both the Tullow pluton and metasedimentary rocks of the Ribband Group.

CHARACTERIZING THE LEINSTER RARE-ELEMENT PEGMATITE BELT AND COUNTRY ROCKS

A recent mineral exploration drilling programme has provided an opportunity to study the Leinster spodumene pegmatites, barren (spodumene-free) pegmatites and their immediate country rocks. The rock types identified in the drill cores in the study areas of Aclare and Moylisha (Fig. 1) are:

(1) Spodumene pegmatite: coarse-grained (crystals up to 10 cm), composed of spodumene (10-40%), albite (25-35%), quartz (15-20%), Li-muscovite (10-15%), spessartine (5%) and minor K-

feldspar, apatite, cassiterite and sphalerite (all less than 5%). Spodumene, albite and Li-muscovite are present as well-formed subhedral crystals, while quartz is interstitial. The dykes can be unzoned, or present zoning when thicker than 10 meters, with an increase in modal spodumene towards the quartz and feldspar core (Fig. 2). In some dykes, crystals of spodumene are aligned perpendicular, and sometimes parallel, to the dyke margins. These observations suggest that each pegmatite dyke has formed by the progressive *in situ* crystallization of a single body of magma. Fine grained albite-rich (85-90%) aplitic patches are common within all zones and include around 10% combined quartz and muscovite, with accessory apatite, cassiterite, spessartine, beryl and Mn,Fe-phosphate.

(2) Barren (spodumene-free) pegmatite: coarse-grained (typically 4 cm, maximum 10 cm), consisting of K-feldspar (10-20%), albite (20-30%), quartz (20-35%), muscovite (15-20%) and spessartine (2-5%). K-feldspar and albite occur as subhedral prismatic crystals, with later quartz and muscovite. Quartz-feldspar intergrowth (graphic texture) is common.

(3) Granodiorite (Leinster Granite): medium-grained granodiorite consisting of quartz (30-45%), oligoclase (30-40%), microcline (10-20%), biotite (5-10%) and muscovite (2-5%), locally porphyritic with occasional 2 cm plagioclase phenocrysts. Sparse tourmaline is observed in some of the contact zones with spodumene pegmatite and its veinlets.

(4) Quartz-mica schist (Ribband Group): fine- to medium-grained schist consisting of biotite (40-50%), muscovite (20-30%), quartz (20-25%) and minor arsenopyrite, titanite and apatite, with a foliation defined by mica; late tourmaline porphyroblasts with poikiloblastic texture are present up to 20 cm from the contact with spodumene pegmatite.

Spodumene pegmatite dykes crosscut both granodiorite and quartz-mica schist in Aclare, and granodiorite only in Moylisha. The contacts between spodumene pegmatite and Leinster Granite are defined by irregular planes and narrow (up to 10 cm) zones of interaction between the two rock types. Contacts between spodumene pegmatite and mica schist are sharp and parallel to the foliation in the mica schist. Spodumene-free pegmatites occur only within granodiorite, against which their contacts are diffuse.

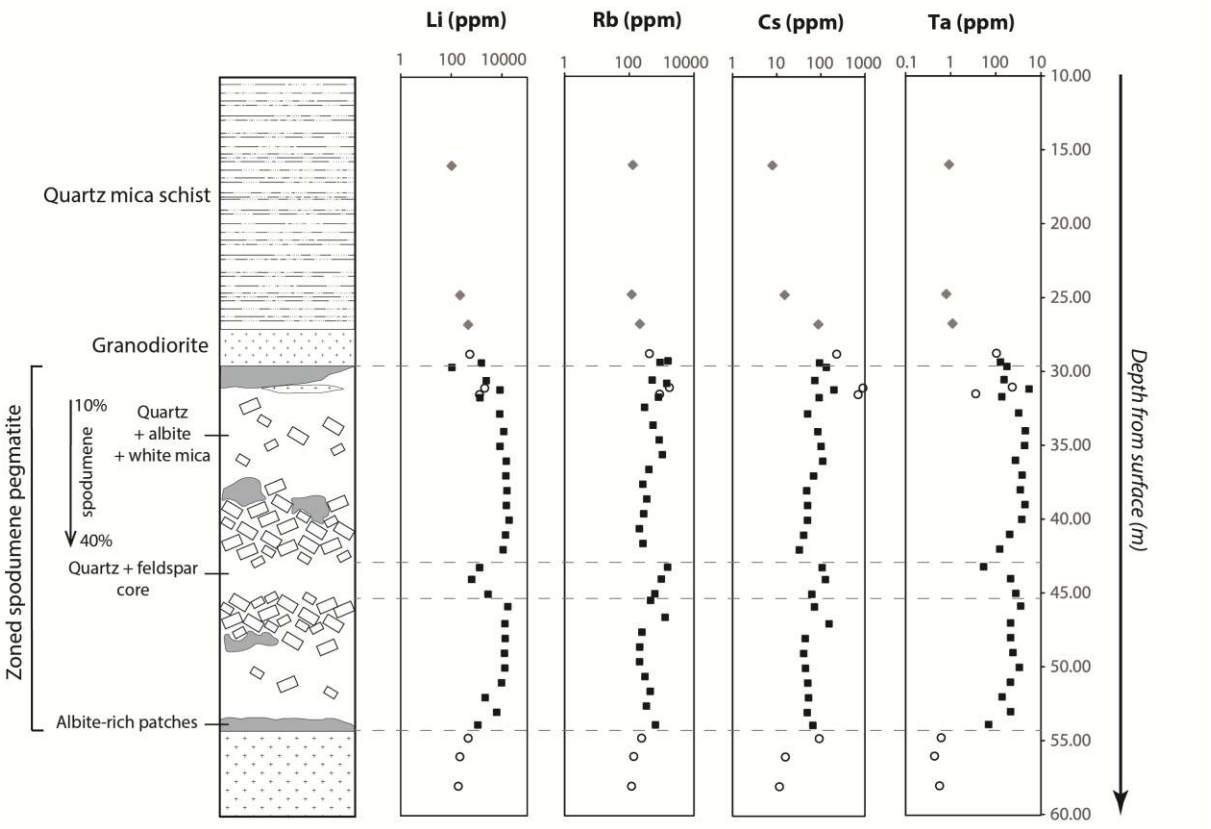

Fig. 2: Mineral and chemical profiles of zoned spodumene pegmatite (drill core ACL13-04). Modal spodumene (open rectangles) increases towards the quartz-feldspar core. Albite-rich aplite occurs as patches throughout the dyke. Whole-rock chemical compositions measured for homogeneous intervals of rock correlate with the mineralogical variation.

METHODS

Sampling and geochemical analysis

Eight mineral exploration drill cores with close to 100% recovery from two localities, Aclare (6 cm diameter) and Moylisha (4 cm diameter), were split in half and divided into homogeneous rock parts, between 7 cm and 3.05 m long, resulting in 281 samples. These parts were then crushed, decomposed using a four acid digestion and analysed for 48 elements by ICP-MS by ALS Minerals (Loughrea, Co. Galway, Ireland). Routine practices were used to ensure data quality control: sample duplicates (1 in every 20 samples), homogeneous quartz pebbles (1/40) and certified standards (1/20). Results showed reproducibility between duplicates within 15% for most elements, except Ta, Zr and Ce, and no contamination problems. Detection limits for the elements analyzed range between 0.002 and 100 ppm. Whole-rock geochemical analysis of pegmatites can be problematic because of their large crystal size, demanding large volume samples for representative results. However, the pegmatites sampled from drill core in the present study have a typical grain size of around 2 cm, with

169 the largest, rare, crystals having grain sizes less than 10 cm, which facilitates representative whole-
170 rock sampling.
171 Pegmatite drill cores were subdivided for whole-rock analysis by lithology into aplite, spodumene-
172 rich pegmatite, pegmatite without spodumene, granodiorite and quartz-mica schist. Weighted mean
173 compositions of each rock type were then calculated for each drill core. For example, in a drill core in
174 which granodiorite constituted a total length of 4.8 m, three samples of lengths 1.6 m, 1.2 m and 2.0 m
175 were analysed. Mean concentrations were then calculated by weighting analyses proportional to the
176 rock volumes in these three core lengths. In the case of pegmatite dykes, the calculation comprised all
177 the intervals from the upper to the lower contact with the country rocks. Contact zones with visible
178 and/or chemical haloes in country rocks and granitic lenses within pegmatites were excluded from the
179 estimated bulk compositions. The method assumes that the drill core samples are representative of the
180 pegmatite bodies as a whole and therefore does not allow for possible chemical variation along strike
181 or down dip within the dykes. It is also assumed that each pegmatite dyke crystallized from a single
182 batch of magma and that bulk pegmatite concentrations of the key elements remained constant during
183 and after crystallization. To highlight possible heterogeneities within rock types between localitites,
184 whole-rock data is presented as the weighted mean of each rock type per drill core, for Aclare and
185 Moylisha separately.
186
187 *Modeling of pegmatite origin by in situ crystallization of granitic magma*
188
189 Calculated bulk concentrations of key elements were used to test whether the Leinster pegmatites
190 could have been derived as a residual phase of continuous crystallization of Leinster Granite
191 granodiorite magma. The elements Ba, Sr, Li, Rb and Cs were chosen as petrogenetic tracers, the first
192 two as compatible elements in granitic minerals and the others as incompatible in granodioritic
193 magma but enriched in pegmatites. To estimate the mean concentrations of these key elements for the
194 Tullow Lowlands pluton, the overall mean of all granitic intervals in all drill cores was considered,
195 weighted by volume as core diameters are different for drill core from Aclare and Moylisha. The same
196 was done for pegmatites and schist, to obtain representative concentrations assuming intrusion of one
197 batch of Li-pegmatite magma and one batch of barren pegmatite magma per dyke.
198 The equation for Rayleigh fractionation has frequently been used for trace element modeling of the
199 formation of pegmatites from granitic magmas (e.g. Shearer *et al.* 1992, Roda-Robles *et al.* 2012).
200 However, the idea of crystals separating from melt through gravity is most likely only applicable to
201 ultramafic melts (Rollinson 1993). In granites and pegmatites solidification most likely starts from the
202 intrusion margins inwards and in pegmatites experimental data suggest that this is a rapid process (*e.g.*
203 Webber *et al.* 1997, 1999, London 2008, Nabelek *et al.* 2010). In this case, a more adequate approach
204 is the quantitative *in situ* crystallization model proposed by Langmuir (1989), in which a solidification
205 zone occurs between the crystallized margins and the central convecting magma batch in a chamber.

Langmuir (1989) considers the case where once solidification starts, all liquid remaining in the solidification front is ultimately separated from the crystal mush and returns to the interior of the magma chamber, which is a reasonable approximation of the current understanding of granite and pegmatite crystallization, and from this assumption the derived equation is $C_L/C_0 = (M_L/M_0)^{(f(D-1)/[D(1-f)+f])}$, where C_L = concentration of the element in the differentiated magma; C_0 = initial concentration of the element in the magma; M_L = mass of the differentiated magma; M_0 = initial mass of the magma chamber; f = fraction of magma allocated to the solidification zone which returns to the unfractionated magma chamber; and D = bulk partition coefficient. The bulk partition coefficient was calculated through the equation $D = \Sigma (X_A Kd_A + X_B Kd_B + X_C Kd_C + \ldots)$, where X_A = weight fraction of mineral A in the rock and Kd_A = mineral A / liquid partition coefficient. This *in situ* crystallization equation also yields the result for simple Rayleigh fractionation, for the condition f =1.

Modeling of pegmatite origin by partial melting

Direct partial melting of a sedimentary source has previously been proposed as an alternative mechanism to form rare element pegmatite magma (*e.g.* Jolliff *et al.* 1992, Shearer *et al.* 1992). The most suitable process to generate the felsic melts discussed is batch melting (Shaw 1970), that can be modelled by the equation $C_L/C_0 = 1/[D_{RS} + F(1 - D_{RS})]$, where C_L = concentration of the element in the generated melt; C_0 = concentration of the element in the unmelted source; D_{RS} = bulk partition coefficient of the residual solid; and F = weight fraction of melt produced. The bulk partition coefficient is calculated in the same way as for the *in situ* crystallization calculations. Minimum PT conditions of partial melting can be estimated based on the minimum temperature of 700 ºC to produce granitic composition melts (MacRae & Nesbitt 1980) and the spodumene stability field, yielding a minimum pressure around 350 MPa. Conditions considered are in agreement with the thermal model for generation of S-type granitic magmas within a transtensional pull-apart zone proposed by Brown *et al.* (2008).

RESULTS

Whole-rock geochemistry

Ranges and means of whole-rock trace and major element concentrations for the four rock types and the relevant study areas are given in Table 1. The granodiorite is classified as peraluminous using the index of Shand (1943) and carries the signature of syn-collisional granites according to the trace element discrimination diagram of Pearce *et al.* (1984) (Fig. 3). Granodiorite in Aclare has lower alkali contents thus higher A/CNK and slightly lower Y and Nb contents when compared to the same rock type in Moylisha. Both types of pegmatites are also peraluminous and syn-collisional, but

spodumene-free pegmatites exhibit the greater scatter in Rb, Y and Nb values. Spodumene pegmatites in Aclare present a high scatter of A/CNK values and higher than Moylisha.

Multi-element diagrams per locality are presented on Fig. 4. Average trace element concentrations for granodiorite show relative abundances decreasing towards the more incompatible elements to the right of the plot and a strong negative Nb anomaly. Spodumene pegmatites and barren pegmatites present a multi-peak signature, with low Ba, Th, La, Ce, Sr and Zr and Y, strong negative Ti anomaly and positive Rb, Ta and Hf anomalies. In comparison with both types of pegmatites, the Leinster Granite granodiorite is enriched in the LIL elements Ba and Sr, which are compatible in feldspars, and in the light rare-earth elements La and Ce.

As Li is a suitable element to differentiate the three granitic rock types (granodiorite, spodumene free pegmatite and spodumene pegmatite), incompatible and compatible elements were plotted against this element (Fig. 5). The three rock types cluster separately without well-defined trends between them. Spodumene pegmatites in Aclare have higher mean Li when compared with the same rock type in Moylisha, while spodumene-free pegmatites in Moylisha present a higher mean Li concentrations than those from Aclare. Granodiorite has the lowest mean Rb concentration and highest mean Sr and Ba, while concentrations of Li and Cs are intermediate between spodumene-free and spodumene pegmatites.

The ratio K/Rb versus Cs is controlled by K-feldspar and micas and is a useful petrogenetic index in granite-pegmatite systems (Černý *et al.* 1981) and values for the studied rock types are shown on Fig. 6. Granodiorites present the highest K/Rb ratios (50-120) and can be locally enriched in Cs as represented by one sample from Aclare. Spodumene pegmatites and barren pegmatites show lower K/Rb ratios of 20-60 and 20-90, respectively. The data do not fit on the expected evolution trend for the case of a parental granite magma fractionating to residual pegmatitic magmas.

Table 1: Geochemical data for the studied rock types in the localities Aclare and Moylisha. Values in ppm. LOD = limit of detection. Duplicate analysis of 15 of the samples shows maximum percentage differences between the higher and lower concentration presented in the last column of the data table.

	LOD (ppm)	Aclare												Moylisha									*Estimation of reproducibility (%)*
		Quartz mica-schist			Granodiorite			Spodumene pegmatite			Spodumene-free pegmatite			Granodiorite			Spodumene pegmatite			Spodumene-free pegmatite			
		mean	min	max	**mean**	min	max	**mean**	min	max	**mean**	min	max	**mean**	min	max	**mean**	min	max	**mean**	min	max	
Li	0.2	**236.8**	97.2	445.1	**395.7**	188.3	569.3	**7020.4**	1678	10794.9	**430.8**	26.8	1076.5	**528.4**	400.3	587.7	**2670.0**	601.8	4144.9	**204.1**	151.4	221.1	*8.1*
Na	100	**11845.9**	10201.8	13752.6	**29734.6**	26516.7	32012.6	**27310.9**	18738.9	40469.7	**37577.1**	33686.3	57400	**26201.9**	25650.1	28160.2	**34556.4**	27540	37405.1	**29523.9**	28480	31939.3	*4.8*
K	100	**24651.7**	24158.2	25449.1	**17492.6**	15403.6	18966.7	**16236.6**	15481.4	17165.2	**24691.2**	4100	35500	**29341.7**	27455.5	30158.6	**21950.7**	16133.4	32401.4	**29939.7**	28562.2	30968.3	*4.9*
Rb	0.1	**150.2**	110.3	205.4	**248.2**	177.4	306.2	**593.1**	496.6	707.8	**725.7**	94.6	1470	**281.1**	245.4	314.2	**559.6**	364	738.9	**361.0**	335.4	371	*8.7*
Cs	0.05	**26.2**	6.6	61.2	**125.1**	30.4	277.4	**77.9**	63.8	99.1	**77.1**	15.6	418	**50.6**	39.4	64.7	**65.5**	45.6	100.8	**36.4**	35.8	36.8	*8.2*
Mg	100	**11176.7**	10687.1	12609.1	**6669.4**	5861.0	7666.7	**262.0**	112.3	933.9	**358.4**	200	400	**4566.0**	3962.2	4840.1	**181.8**	80	381.3	**696.3**	624.7	724.6	*5.4*
Ca	100	**3786.0**	2664.3	5370.6	**14090.5**	6366.7	17842.0	**1787.3**	969.7	6408.9	**1760.6**	1366.5	3200	**12189.2**	10457.1	12784.3	**1130.6**	799.9	1791.4	**3436.8**	3086.7	3553.9	*10.2*
Sr	0.2	**119.8**	95.1	153.7	**227.0**	133.9	281.1	**15.3**	12	29.1	**16.3**	9.5	40.4	**158.6**	137.1	171.6	**16.3**	11	29.9	**35.3**	27.6	38.5	*10.0*
Ba	10	**499.9**	482.1	520	**335.0**	279.2	357.3	**16.7**	9.7	35.9	**36.4**	20	50	**368.2**	321.0	378.3	**15.3**	8.4	32.9	**60.6**	59.3	62.3	*6.9*
Ti	50	**4585.7**	4323.3	5016.9	**2094.2**	2066.7	2178.6	**11.1**	2.9	32.6	**6.0**	0	100	**2211.5**	1914.2	2308.9	**33.5**	13.3	116.3	**290.1**	221.6	335.6	*2.9*
Mn	5	**696.8**	495.2	1190.3	**500.2**	416.4	590.9	**935.6**	741.4	1009.6	**302.6**	108	649	**565.6**	499.0	584.7	**783.5**	656.2	1041.1	**761.7**	636	902.9	*8.0*
Fe	100	**48192.0**	46395.4	50366.7	**20568.5**	19728.1	21000.9	**4316.3**	3513.3	4600	**4152.4**	2100	4863.1	**17271.1**	15905.3	17838.6	**3292.2**	2863.8	4007.1	**5952.1**	5775	6145.5	*10.2*
Y	0.1	**15.9**	14.8	18.1	**6.4**	5.7	7.1	**0.3**	0.1	1.5	**0.6**	0.5	0.8	**8.2**	7.8	8.4	**0.4**	0.1	2.5	**4.8**	3.2	6.3	*13.3*
Zr	0.5	**105.0**	97.6	115.2	**37.1**	34.7	40.6	**12.0**	9.2	15	**12.2**	7.6	23.2	**97.5**	77.2	105.3	**13.4**	7.8	20	**21.0**	19	22	*15.9*
Nb	0.1	**13.9**	13.3	14.2	**6.7**	5.3	7.2	**28.0**	24.1	33.5	**33.8**	11.1	109.5	**8.0**	7.3	8.3	**34.3**	22.1	45.2	**10.3**	9.8	11.1	*7.0*
Hf	0.1	**3.0**	2.7	3.2	**1.2**	1.2	1.3	**1.4**	1.2	1.8	**1.4**	1	3	**2.8**	2.4	3.2	**2.1**	1.4	2.7	**1.2**	1.1	1.2	*8.7*
Ta	0.05	**1.0**	0.9	1.1	**2.5**	0.5	3.4	**27.6**	17.9	50.1	**36.2**	16.3	180	**1.7**	1.3	1.9	**33.9**	20.9	44.2	**4.4**	4.1	5.1	*26.4*
Al	100	**86710.3**	84007.1	89132.5	**75597.8**	69600.0	78509.0	**68487.7**	65249.5	70403	**68118.4**	50800	78300	**74074.3**	73271.9	74682.2	**63341.4**	53760.2	71578.5	**67780.4**	64332.3	71249.3	*7.2*
P	10	**427.5**	384.3	494.9	**557.6**	375.8	655.3	**669.0**	489.1	1038.9	**677.4**	430	1530	**864.6**	751.3	922.6	**503.4**	386.4	745.1	**537.3**	461.9	659.6	*5.5*
La	0.5	**33.9**	32.7	35.9	**13.9**	12.1	14.9	**0.2**	0	1	**0.3**	0.1	0.7	**25.7**	21.6	27.9	**0.2**	0	0.9	**3.8**	2.6	4.6	*8.8*
Ce	0.01	**73.0**	71.6	74.6	**28.4**	23.9	29.8	**0.7**	0.4	2.2	**1.0**	0.8	1.4	**57.3**	48.2	60.9	**0.6**	0.2	2.2	**8.5**	6	10.4	*40.1*
Th	0.2	**10.5**	9.2	11.4	**4.9**	4.7	5.6	**0.6**	0.5	0.8	**0.9**	0.4	3.1	**11.5**	9.4	12.2	**2.6**	2.3	3	**2.5**	1.8	3	*13.3*

Values indicate minimum and maximum concentrations calculated for rock types in each drill core and the mean value is calculated as the mean of all analysed samples from each locality weighted by volume. The volumes of core that contributed to these calculated mean concentrations are: quartz-mica schist – Aclare and total 0.075 m^3; granodiorite – Aclare 0.11 m^3, Moylisha 0.13 m^3, total 0.24 m^3; spodumene pegmatite – Aclare 0.15 m^3, Moylisha 0.05 m^3, total 0.20 m^3; spodumene-free pegmatite – Aclare 0.02 m^3, Moylisha 0.04 m^3, total 0.06 m^3.

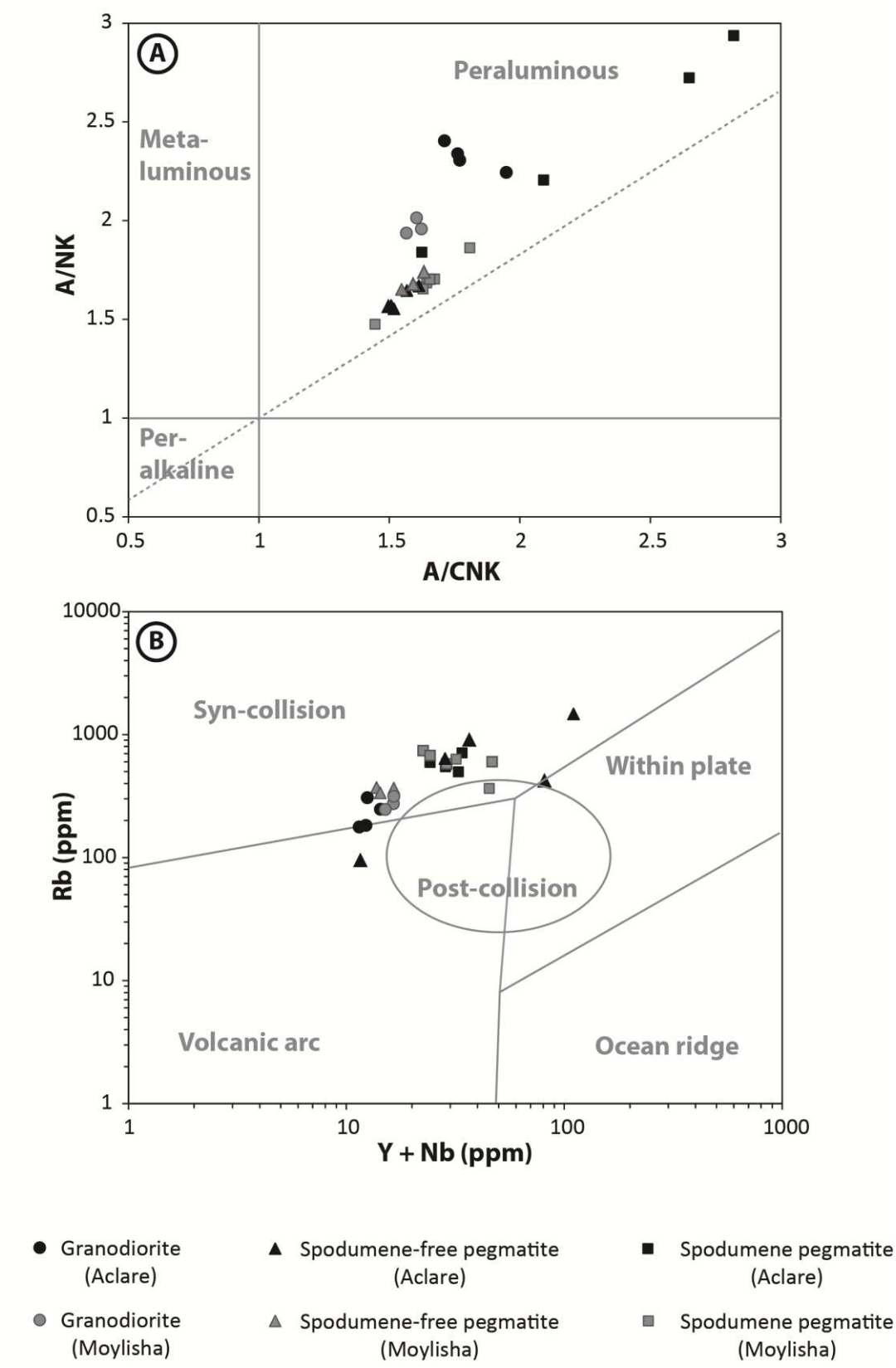

Fig. 3: A) A/CNK versus A/NK plot (Shand 1943) showing the peraluminous character of granodiorite and pegmatites. B) Trace element discrimination diagram of Pearce *et al.* (1984) showing

277 syn-collisional signature of the rock types. Data points represent mean concentrations weighted by
278 drill core volume of each rock type in individual drill cores.

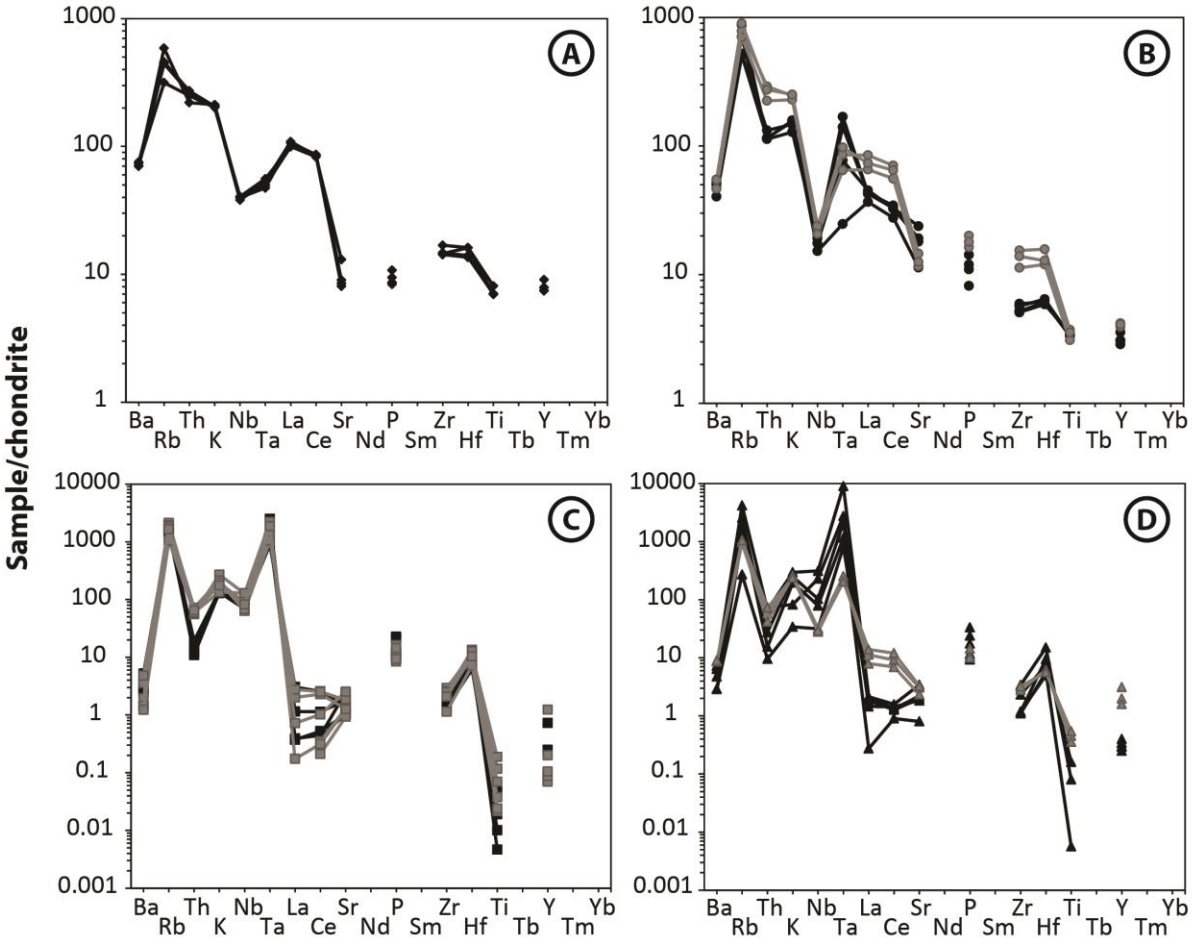

279

280 Fig. 4: Trace element concentrations are normalized to the composition of chondritic meteorites given
281 by Thompson (1982). Samples in black are from Aclare and in grey from Moylisha. The diagrams are
282 for A) quartz-mica schist; B) granodiorite; C) spodumene pegmatites and D) spodumene-free
283 pegmatites. Gaps indicate no available data.

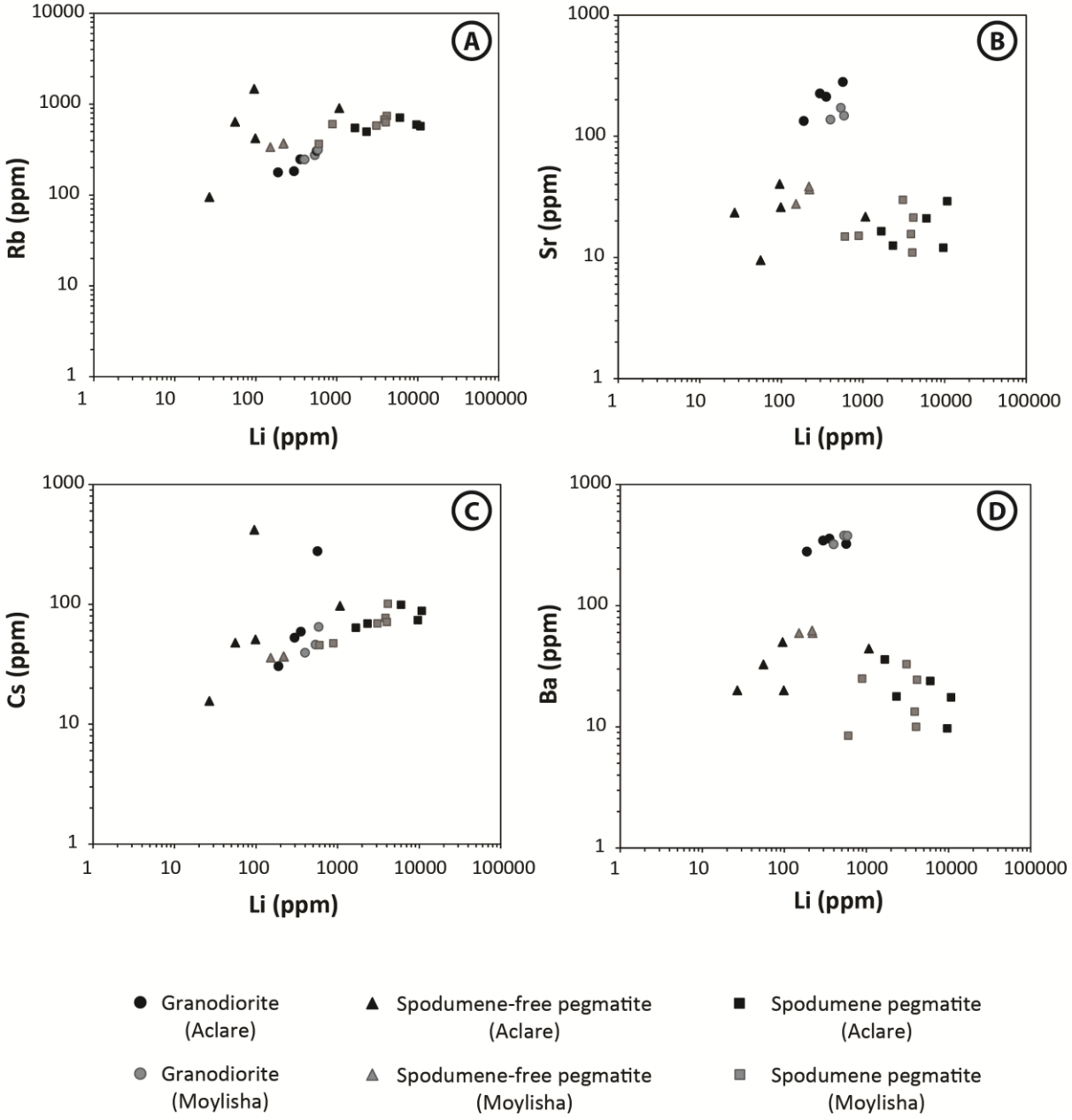

284

285 Fig. 5: Bivariate plots of Li versus A) Rb, B) Sr, C) Cs and D) Ba. Samples in black are from Aclare
286 and in grey from Moylisha.

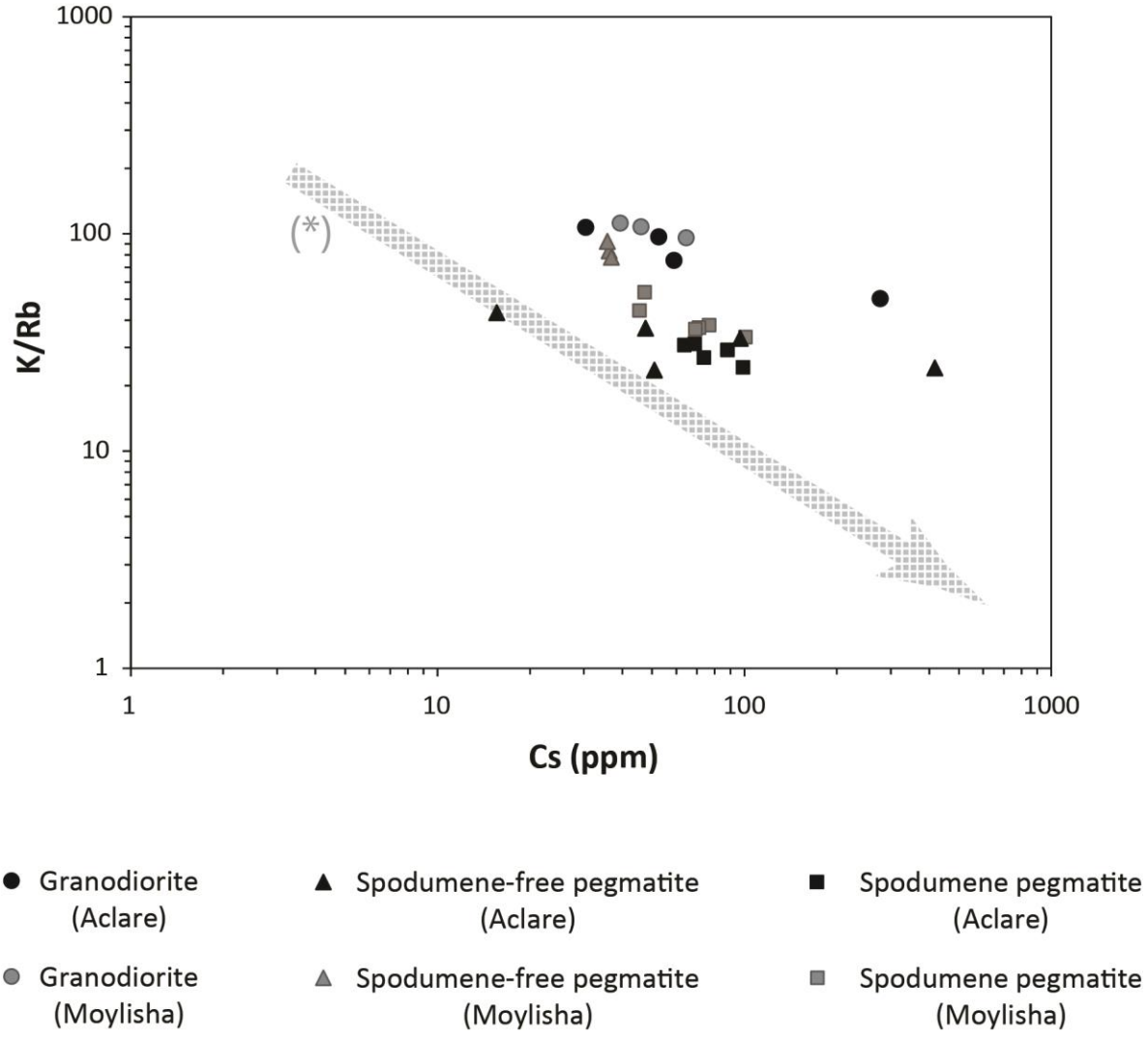

Fig. 6: Cs versus K/Rb as an index of chemical evolution of pegmatites. (*) For comparison, the arrow indicates data presented in London (2008) for variation within a granite-pegmatite group (Red Cross Lake, Manitoba) with a proven petrogenetic link.

Partition coefficients used in modeling

Modeling of both *in situ* crystallization and batch melting requires calculation of bulk partition coefficients. As already debated in other pegmatite modeling studies (e.g. Jolliff *et al.* 1992, Shearer *et al.* 1992), uncertainty of the appropriate values of bulk partition coefficients can arise for several reasons. Several variables can affect mineral/melt partition coefficients, including temperature, confining pressure and melt composition (Rollinson 1993), but none of these are considered to be major issues in the studied granite-pegmatite systems. The partition coefficients and their published sources chosen for the key elements in granitic and pegmatitic minerals are presented in Table 2. Values were chosen to be representative of high-Si crystallizing magmas, consistent with the predominant granodiorite in Leinster Granite, and maximum values available were used for

303 calculations in cases where the reference presented a range. Bulk partition coefficients were
304 calculated considering the mineral assemblages discussed below.
305
306 Table 2: Crystal / melt partition coefficients used for quantitative modeling.

Mineral/melt	Albite	Muscovite	Quartz & aluminosilicate	K-feldspar	Biotite
Li	0.1	1.67	0.05	0.05	1.65
reference	*9*	*3*	*8*	*9*	*3*
Rb	0.06	1.75	0.016	0.74	5.3
reference	*6*	*3*	*7*	*1*	*1*
Cs	0.44	0.24	0.044	0.13	3.1
reference	*6*	*3*	*7*	*2*	*1*
Sr	3.31	0.5	0.01	5	0.06
reference	*4*	*3*	*assumed*	*5*	*3*
Ba	0.19	5.5	0.015	6.7	7
reference	*6*	*3*	*7*	*1*	*1*

References: 1 Mahood & Hildreth (1983); 2 Icenhower & London (1996); 3 Icenhower & London (1995); 4 Drake & Weill (1975); 5 Long (1978); 6 Bea *et al.* (1994); 7 Nash & Crecraft (1985); 8 Jollif *et al.* (1992); 9 Walker *et al.* (1989).

307
308
309 *In situ crystallization modeling*
310
311 *In situ* crystallization calculations test the hypothesis that pegmatites and granodiorite are
312 genetically linked through a continuous evolution model in a closed system (Fig. 7). Whole-rock
313 concentrations of Li, Rb, Cs, Sr and Ba were estimated for granodiorite, spodumene pegmatite, barren
314 pegmatite and schist as means weighted by total drill core volume of all analyses from all drill cores,
315 for each rock type. These means for granodiorite are then considered to represent the initial magma
316 from which residual pegmatitic fluids might have evolved in the late stages of crystallization, and
317 subsequently escaped to be intruded as dykes; concentrations for schist are presented for comparison
318 only in this scenario. Fractionation paths with various combinations of parameters were calculated, to
319 show whether it is possible to reach bulk concentrations for the residual magma that are similar to
320 mean spodumene pegmatite and barren pegmatite chemical compositions. The crystallizing
321 assemblage considered is plagioclase (40%), K-feldspar (25%), quartz (25%), biotite (5%) and white
322 mica (5%).
323 In *in situ* crystallization, the enrichment of a trace element in the residual melt relative to the
324 parent melt (C_L/C_0) varies according to the mass of residual melt relative to the total mass of the
325 magma chamber (M_L/M_0), the fraction of liquid returned to the main magma body from the

326 solidification zone (f) and the bulk partition coefficient (D). From lithogeochemical data, the values of
327 C_0 were considered to be the bulk trace element concentration calculated for granodiorite as the initial
328 magma. The fraction M_L/M_0 is equivalent to the fraction of residual magma and values between 0.01
329 (99% residual magma, start of crystallization) and 0.99 (1% residual magma, end of crystallization)
330 were considered. Values of f range between 0.01 (1% liquid returned from solidification zone,
331 representing very rapid crystallization) and 1 (all liquid returns from the solidification zone,
332 representing Rayleigh fractionation). The bulk partition coefficient, and therefore different values of
333 partition coefficients for the elements studied, can contribute substantially to variations in the final
334 result and this will be discussed later.
335 The ranges of possible enrichment and depletion of the five key elements, with granodiorite as
336 model initial magma, are plotted on Fig. 8. Average concentrations for key elements in pegmatites are
337 not always within the ranges of possible concentrations reached by *in situ* crystallization and the
338 maximum limiting Rayleigh fractionation. The magnitude of depletion in Ba and Sr and enrichment in
339 Rb and Li by *in situ* crystallization is sufficient to reach the mean composition of spodumene
340 pegmatite. However, very different crystallization conditions are required to individually explain the
341 elements analysed; for example ~95% crystallization at f ~0.8 can produce mean spodumene
342 pegmatite composition on the Ba-Li plot, whereas at least 99% crystallization is required at f ~0.3 to
343 produce mean spodumene pegmatite on the Rb-Li plot; there are no conditions which can account for
344 the mean Cs concentration of the spodumene pegmatites. Spodumene-free pegmatite compositions are
345 even less well reproduced by in situ crystallization (Fig. 8).
346

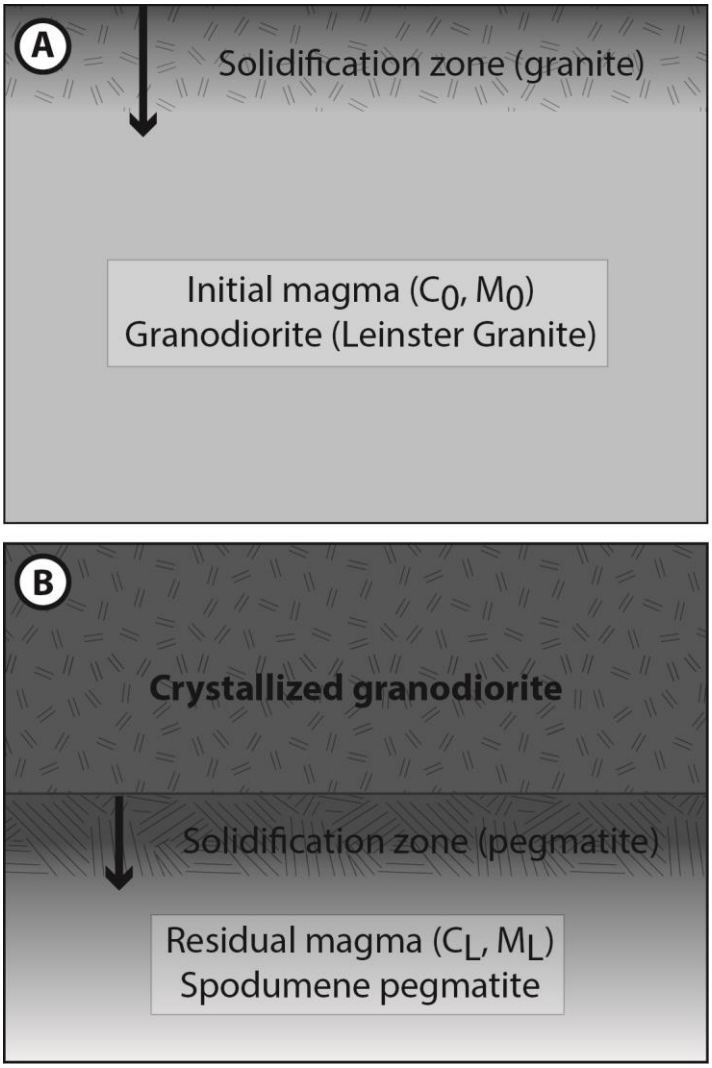

Fig. 7: *In situ* crystallization model (Langmuir 1989) applied to the Leinster Granite granodiorite - pegmatites system, depicting continuous granodiorite-to-pegmatites evolution within the same magma batch. A) Solidification starts from the margins of the magma chamber inwards, with a fraction of magma returning to the main magma body. The initial magma's composition is equivalent to the bulk composition of the crystallized granodiorite. B) After extensive crystallization, the residual magma would have become concentrated in incompatible elements and have a composition equivalent to the most evolved bulk spodumene pegmatite dykes. The same process could also generate the (less evolved) spodumene-free pegmatites as an intermediate member or as another end-member.

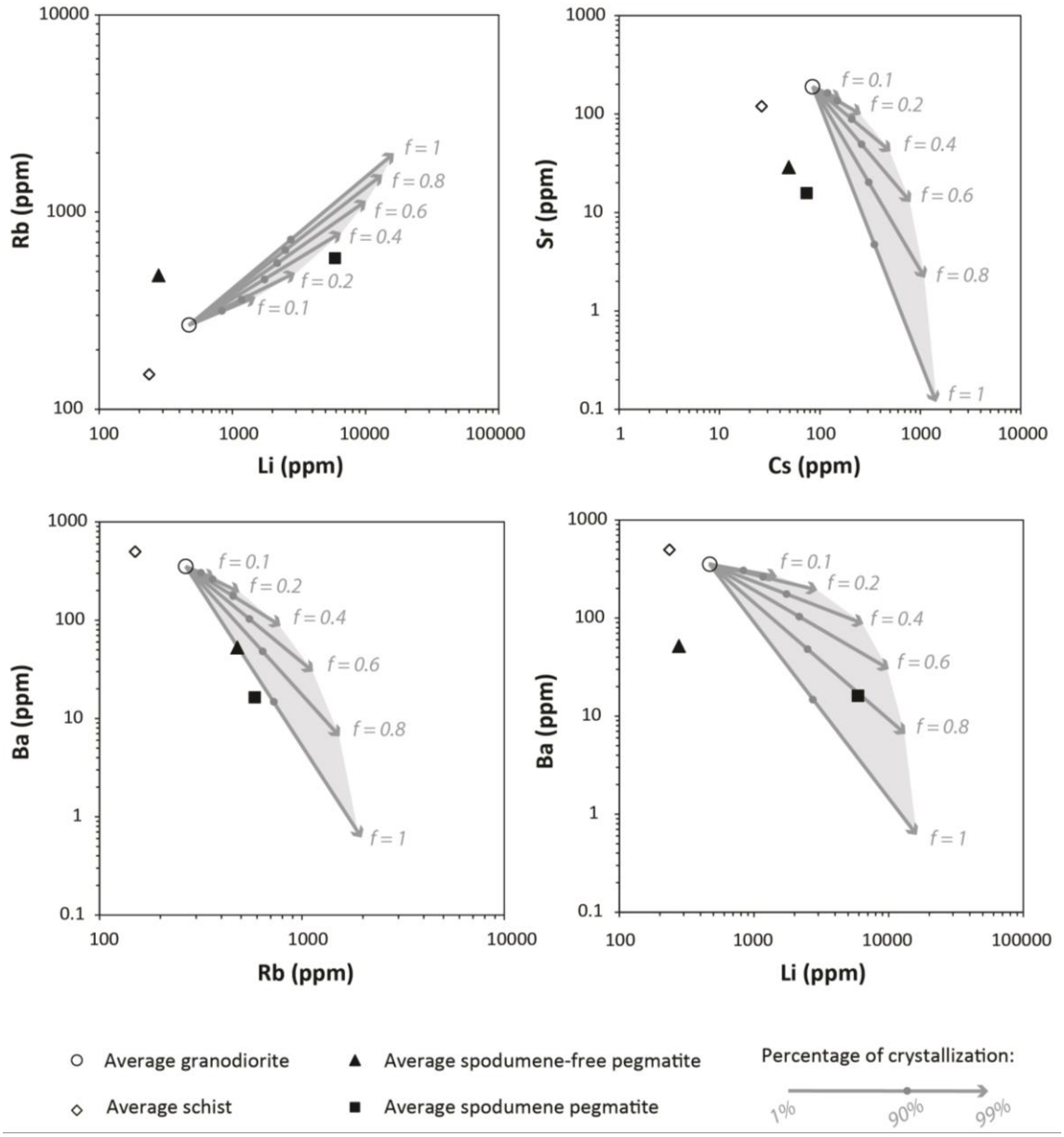

Fig. 8: Bivariate plots with the results of *in situ* crystallization modeling with the average Leinster Granite granodiorite as the initial magma. The arrows show the range from minimum (10%) to maximum (100%) fractions of liquid returned (f) to the main magma body from the solidification zone considered in this system – 100% returned is equivalent to Rayleigh fractionation. The grey area shows the range of values with other values of f between 0.1 and 1.

Batch melting modeling

The range of suitable initial compositions of sedimentary sources that underwent batch partial melting forming the three rock types were also calculated to assess whether a common origin for them is possible. In batch melting, the concentration of an element in the generated melt compared with the concentration of the element in the unmelted source (C_L/C_0) varies with the weight fraction of melt

produced (F) and the bulk partition coefficient of the residual solid in the source (D_{RS}). The weighted mean concentrations measured in the three rock types were considered as different values for C_L, allowing calculation of the range of necessary concentrations in the source C_0 to generate melts with the measured compositions. The range of initial concentrations was calculated from 1% melting (F = 0.01) to 99% melting (F = 0.99). In order to calculate D_{RS}, the source was estimated to be quartz feldspar-rich sediment, since partial melting of pelitic sediments would result in Li, Rb and Cs being retained in the mica-rich residual solid as partition coefficients are high for these elements (Jolliff *et al.* 1992 and references therein). The residual solid considered would be mainly composed of quartz (25%), feldspars (50%) and aluminosilicate (25%), thus allowing for all mica to be melted. Variations in the percentages of these minerals in the residual solid and from the partition coefficients chosen do not have major impact on the final results.

Possible initial concentrations in sources that can form melts with the compositions of average granodiorite and pegmatites are featured on Fig. 9. Considering a range of 1 to 40% of partial melting to form the three rock types (1 to 10% for pegmatites and 10 to 40% for granodiorite), the lines of initial concentrations converge to a restricted area representing little variation in the source for Rb (50 to 130 ppm), Li (30 to 430 ppm) and Cs (around 10 ppm). For Ba and Sr, initial concentrations converge to restricted areas for pegmatites (30 to 90 ppm Ba, 30 to 60 ppm Sr), but indicate a source more enriched in those elements for granodiorite (around 600 ppm Ba and 400 ppm Sr).

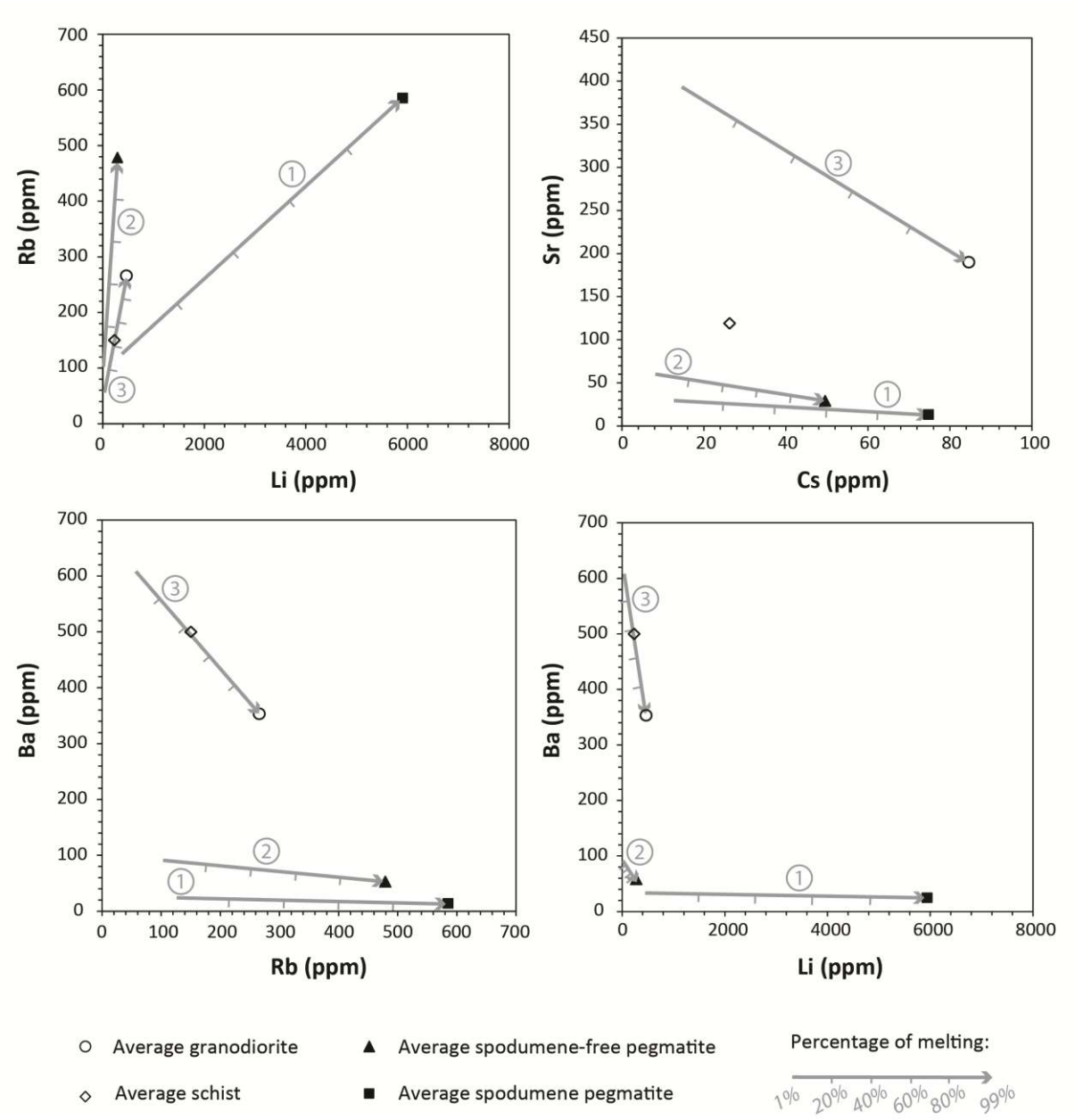

Fig. 9: Bivariate plots with the results of partial melting modeling. The arrows show the possible initial concentrations of the magma source rocks for spodumene pegmatite (line 1), spodumene-free pegmatite (line 2) and granodiorite (line 3) if they underwent 1 to 99% melting. Average composition of the schist is plotted for comparison, representing metasedimentary rocks of the Ribband Group.

IMPLICATIONS FOR SPODUMENE PEGMATITE FORMATION

The strong negative Nb anomaly in Leinster Granite granodiorite indicates that a crustal component is involved in its formation, which can also be inferred for pegmatites, but with a less pronounced negative anomaly. Pegmatites do not always carry higher concentrations of incompatible elements than granodiorite (e.g. concentrations of Zr, Ti and Y) and no clear fractionation trends are observed among incompatible or compatible elements, or ratios that indicate chemical evolution.

Plotted geochemical data is scattered rather than representing a chemically closed or semi-closed continuous evolution system. Although the key elements Li and Cs have not been analysed in samples from elsewhere in the Leinster Granite, the chemical signature of granodiorites within the batholith varies between localities, probably reflecting the multi-intrusion character of the batholith and some variation in source rock composition (Mohr 1991, Sweetman 1987, Grogan & Reavy 2002).

With the chosen partition coefficients it is not possible to reach spodumene pegmatite mean concentration considering all elements, therefore a single crystallizing system from granodiorite to pegmatite. If, however, the bulk partition coefficient for Ba (D_{Ba}) is double that listed in Table 2, by consequence of higher $Kd_{Ba}^{biotite/liquid}$ and $Kd_{Ba}^{K\text{-}feldspar/liquid}$, the required depletion of this element from granodiorite to pegmatites can be attained. Such high values were obtained experimentally by Icenhower & London (1996), for example. For Rb, a slightly lower bulk partition coefficient makes possible the enrichment observed in spodumene pegmatites. This would be mainly controlled by a lower $Kd_{Rb}^{biotite/liquid}$ and such lower values have been obtained experimentally (*e.g.* Icenhower & London 1995). However, the spodumene pegmatite Sr and Cs concentrations cannot be reached using reasonable partition coefficients for these elements. They could only be reached with a much higher Cs bulk partition coefficient. Extreme Li concentrations found in spodumene pegmatite can be reached towards high fraction of magma return from the solidification front, or Raleigh fractionation, and with less than 5% magma left, but this scenario would require the combination of cumulate-type crystallization followed by effective extraction of the residual magma. Therefore granodiorite-to-pegmatite magmatic evolution seems highly unlikely taking account of all five elements.

One possibility to explain the discrepancy observed when trying to correlate concentrations of key elements through the Langmuir *in situ* crystallization equation is a significant loss of the mobile elements Rb, Cs and Li at some stage between generation, ascent and emplacement of pegmatite magma. However, very narrow exomorphic haloes (up to 20 cm) into the granodiorite and the permeable quartz-mica schist do not support this hypothesis. Cs mobility does however seem possible as high-Cs granodiorite is observed (Figs. 5 and 6). The mean Cs concentration for the initial magma could be lower if this locally high-Cs granodiorite is considered to be part of an exomorphic halo (and therefore excluded from bulk composition calculations), but still considerably higher D_{Cs} would be needed to reach pegmatite concentrations. Another possibility is contamination from country rocks, especially contamination of spodumene pegmatites by the schist, but its mean composition with low Li (<250 ppm), Rb (<150 ppm) and Cs (<30 ppm) cannot explain the deviations of *in situ* crystallization trends away from pegmatite compositions.

On the other hand, with a narrow range of high source rock incompatible element concentrations and reasonable assumptions for degrees of partial melting, it is possible to form melts with the average composition of granodiorite, spodumene-free and spodumene pegmatites. However, source compatible element concentrations have to be highly variable if the three lithologies share a common source. As bulk concentrations of Ba and Sr would strongly depend on the amount of feldspars in

metasedimentary rocks, this variation can be explained by the presence of feldspar-rich and feldspar-poor source rocks, generating granodiorite and pegmatites, respectively. If pegmatite magmas were generated at the same time or later than the granodioritic magmas that formed the Leinster Granite, as implied by cross-cutting relationships, the required source rock heterogeneity likely existed on at least a kilometre scale. Otherwise, it is difficult to envisage the pegmatite source rocks remaining unmelted during Leinster Granite granodiorite magma formation.

CONCLUSIONS AND FUTURE WORK

Observing patterns on multi-element diagrams and bivariate plots, the behaviour of incompatible elements and the absence of fractionation trends among elements, the hypothesis that pegmatite magmas formed by the continuous evolution of the same magmatic system as the Leinster Granite granodiorite is not a satisfactory explanation for the origin of these rocks. Specifically, *in situ* crystallization modeling shows that it is highly unlikely that pegmatites represent the residual magma from crystallization of Leinster Granite granodiorite. This requires that granodiorite and pegmatite magmas were derived in separate partial melting events, the pegmatites presumably representing a later event because they are observed to intrude granodiorite. However the source rocks required to account for the geochemistry of pegmatites and the Leinster Granite granodiorite must be different, with considerably more feldspar required in the granodiorite source rocks than in the pegmatites' source rocks. An unresolved question is why magmas that formed igneous rocks in close spatial association (granodiorite plutons and pegmatite dykes) were not apparently formed by partial melting of the same source rocks. In an alternative scenario the voluminous Leinster Granite could represent mixing between mantle-derived mafic magma and crustal melts of similar rocks that alone generated pegmatite magmas. Precise dating and radiogenic isotope studies to define the sources are planned towards a better understanding of the story behind the formation of pegmatites in southeast Ireland.

ACKNOWLEDGEMENTS

The authors would like to thank two anonymous reviewers for their suggestions that improved the quality of this manuscript; Mr. John Harrop, Dr. Mark Holdstock, Mr. Patrick McLaughlin, Mr. Graham Parkin and Ms. Emma Sheard, as well as the whole team of Blackstairs Lithium Ltd., for helpful discussions, for providing access to drill core and lithogeochemical data and for the permission to publish it; Mr. Tom Culligan for thin sectioning; CAPES/Science Without Borders (BEX 9548/13-0) for the financial support. This publication has emanated from research supported in part by a research grant from Science Foundation Ireland (SFI) under Grant Number 13/RC/2092 and co-funded under the European Regional Development Fund.

REFERENCES

BEA, F., PEREIRA, M.D. & STROH, A. (1994) Mineral/leucosome trace-element partitioning in a peraluminous migmatite (a laser ablation-ICP-MS study). *Chemical Geology* **117**, 291-312.

BRINDLEY, J.C. (1973) The structural setting of the Leinster Granite, Ireland. Scientific Proceedings of the Royal Dublin Society A**5**, 27-36.

BROWN, P.E., RYAN, P.D., SOPER, N.J. & WOODCOCK, N.H. (2008) The Newer Granite problem revisited: a transtensional origin for the Early Devonian Trans-Suture Suite. *Geological Magazine* **145**(2), 235-256.

ČERNY, P., TRUEMAN, D.L., ZIEHLKE, D.V., GOAD, B.E. & PAUL, B.J. (1981) The Cat Lake – Winnipeg River and the Wekusko Lake pegmatite fields, Manitoba. *Manitoba Department of Energy and Mines, Mineral Resources Division, Economic Geology Report* **ER80-1**.

ČERNY, P., TEERTSTRA, D.K., CHAPMAN, R., SELWAY, J.B., HAWTHORNE, F.C., FERREIRA, K., CHACKOWSKY, L.E., WANG, X. & MEINTZER, R.E. (2012) Extreme fractionation and deformation of the leucogranite-pegmatite suite at Red Cross Lake, Manitoba, Canada. *The Canadian Mineralogist* **50,** 1839-1875.

DRAKE, M.J. & WEILL, D.F. (1975) Partition of Sr, Ba, Ca, Y, Eu^{2+}, Eu^{3+}, and Other REE between plagioclase feldspar and magmatic liquid - experimental study. *Geochimica et Cosmochimica Acta* **39**(5), 689-712.

GRAHAM, J.R. & STILLMAN, C.J. (2009) Ordovician of the south. *In:* Holland, C.H. & Sanders, I. [*eds.*] The geology of Ireland, 2nd edition, 568p.

GROGAN, S.E. & REAVY, R.J. (2002) Disequilibrium textures in the Leinster Granite Complex, SE Ireland: evidence for acid-acid magma mixing. *Mineralogical Magazine* **66**(6), 929-939.

HOLLAND, C.H. (2009) Silurian. *In:* Holland, C.H. & Sanders, I. [*eds.*] The geology of Ireland, 2nd edition, 568p.

ICENHOWER, J. & LONDON, D. (1995) An experimental study of element partitioning among biotite, muscovite, and coexisting peraluminous silicic melt at 200 MPa (H_2O). *American Mineralogist* **80**, 1229-1251.

ICENHOWER, J. & LONDON, D. (1996) Experimental partitioning of Rb, Cs, Sr, and Ba between alkali feldspar and peraluminous melt. *American Mineralogist* **81**, 719-734.

JOLLIFF, B.L., PAPIKE, J.J. & SHEARER, C.K. (1992) Petrogenetic relationships between pegmatite and granite based on geochemistry of muscovite in pegmatite wall zones, Black Hills, South Dakota, USA. *Geochimica et Cosmochimica Acta* **56,** 1915-1939.

LANGMUIR, C.H. (1989) Geochemical consequences of *in situ* crystallization. *Nature* **340**(6230), 199-205.

LONDON, D. (2008) Pegmatites. *Canadian Mineralogist, Special Publication* 10, 347p.

LONG, P.E. (1978) Experimental determination of partition coefficients for Rb, Sr, and Ba between alkali feldspar and silicate liquid. *Geochimica et Cosmochimica Acta* **42**, 833-846.

MACRAE, N.D. & NESBITT, H.W. (1980) Partial melting of common metasedimentary rocks: a mass balance approach. *Contributions to Mineralogy and Petrology* **75**(1), 21-26.

MAHOOD, G. & HILDRETH, W. (1983) Large partition coefficients for trace elements in high-silica rhyolites. *Geochimica et Cosmochimica Acta* **47,** 11-30.

MCARDLE, P. & KENNEDY, M.J. (1985) The East Carlow Deformation Zone and its regional implications. *Geological Survey of Ireland Bulletin* **3**(4), 237-255.

MCCONNELL, B.J, & PHILCOX, M.E. (1994) Geology of Kildare-Wicklow, a geological description to accompany the bedrock geology 1:100,000 map series, Sheet 16, Kildare-Wicklow. *Geological Survey of Ireland*, 70p.

MOHR, P.J. (1991) Cryptic Sr and Nd isotopic variation across the Leinster Granite, southeast Ireland. *Geological Magazine* **128**(3), 251-256.

MULLER, A, IHLEN, P.M., SNOOK, B., LARSEN, R.B., FLEM, B., BINGEN, B. & WILLIAMSON, B.J. (2015) The chemistry of quartz in granitic pegmatites of southern Norway: petrogenetic and economic implications. *Economic Geology* **110,** 1737-1757.

547 NABELEK, P.I., WHITTINGTON, A.G. & SIRBESCU, M.C. (2010) The role of H_2O in rapid emplacement
548 and crystallization of granitic pegmatites: resolving the paradox of large crystals in highly
549 undercooled melts. *Contributions to Mineralogy and Petrology* **160,** 313-325.
550
551 NASH, W.P. & CRECRAFT, H.R. (1985) Partition coefficients for trace elements in silicic magmas.
552 *Geochimica et Cosmochimica Acta* **49**, 2309-2322.
553
554 O'CONNOR, P.J., AFTALION, M. & KENNAN, P.S. (1989) Isotopic U-Pb ages of zircon and monazite
555 from the Leinster Granite, Southeast Ireland. *Geological Magazine* **126**(6), 725-728.
556
557 O'CONNOR, P.J., GALLAGHER, V. & KENNAN, P.S. (1991) Genesis of lithium pegmatites from the
558 Leinster Granite margin, southeast Ireland: geochemical constraints. *Geological Journal* **26**, 295-305.
559
560 PEARCE, J.A., HARRIS, N.B.W. & TINDLE, A.G. (1984) Trace element discrimination diagrams for the
561 tectonic interpretation of granitic rocks. *Journal of Petrology* **25**(4), 956-983.
562
563 RODA-ROBLES, E., PESQUERA, A., GIL-CRESPO, P. & TORRES-RUIZ, J. (2012) From granite to highly
564 evolved pegmatite: a case study of the Pinilla de Fermoselle granite-pegmatite system (Zamora,
565 Spain). *Lithos* **153,** 192-207.
566
567 ROLLINSON, H. (1993) Using geochemical data: evaluation, presentation, interpretation, 1st edition.
568 *The Longman Geochemistry Series,* 352p.
569
570 SHAND, S. J. (1943) The Eruptive Rocks, 2nd edition. New York: John Wiley, 444 p.
571
572 SHAW, D.M. (1970) Trace element fractionation during anatexis. *Geochimica et Cosmochimica Acta*
573 **34,** 237-243.
574
575 SHEARER, C.K., PAPIKE, J.J. & JOLIFF, B.L. (1992) Petrogenetic links among granites and pegmatites
576 in the harney peak rare-element granite-pegmatite system, Black Hills, South Dakota. *The Canadian*
577 *Mineralogist* **30,** 785-809.
578
579 STEIGER, R. (1977) Prospecting for lithium and tungsten in Ireland. *In: Prospecting in areas of*
580 *glaciated terrain*, Helsinki Institution of Mining and Metallurgy, 14-24.
581
582 STEIGER, R. & VON KNORRING, O. (1974) A lithium pegmatite belt in Ireland. *Journal of Earth*
583 *Sciences, Leeds Geological Association* **8,** 433-443.

SWEETMAN, T.M. (1987) The geochemistry of the Blackstairs Unit of the Leinster Granite, Ireland. *Journal of the Geological Society, London* **144,** 971-984.

THOMPSON, R.N. (1982) Magmatism of the British Tertiary Volcanic Province. *Scottish Journal of Geology* **18,** 49-107.

VILLA, I.M., DE BIÈVRE, P., HOLDEN, N.E. & RENNE, P.R. (2015) IUPAC–IUGS recommendation on the half life of ^{87}Rb. *Geochimica et Cosmochimica Acta* **164,** 382–385.

WALKER, R.J., HANSON, G.N. & PAPIKE, J.J. (1989) Trace element constraints on pegmatite genesis: Tin Mountain pegmatite, Black Hills, South Dakota. *Contributions to Mineralogy and Petrology* **101,** 290-300.

WEBBER, K.L., FALSTER, A.U., SIMMONS, W.B. & FOORD, E.E. (1997) The role of diffusion-controlled oscillatory nucleation in the formation of Line Rock in pegmatite-aplite dikes. *Journal of Petrology* **38**(12), 1777-1791.

WEBBER, K.L., SIMMONS, W.B., FALSTER, A.U. & FOORD, E.E. (1999) Cooling rates and crystallization dynamics of shallow level pegmatite-aplite dikes, San Diego County, California. *American Mineralogist* **84**, 708-717.

WHITWORTH, M.P. (1992) Petrogenetic implications of garnets associated with lithium pegmatites from SE Ireland. *Mineralogical Magazine* **56,** 75-83.

WHITWORTH, M.P. & RANKIN, A.H. (1989) Evolution of fluid phases associated with lithium pegmatites from SE Ireland. *Mineralogical Magazine* **53,** 271-284.